

DOE/ER/20719-2

**SPECTROSCOPIC DIAGNOSTICS on  
HIGH-DENSITY, STRONGLY-COUPLED ICF PLASMAS**

**Final Report  
February 1, 1995 - November 30, 1995**

**Hans R. Griem, Raymond C. Elton and Benjamin L. Welch**

**University of Maryland  
College Park, MD 20742-3511**

**DISCLAIMER**

This report was prepared as an account of work sponsored by an agency of the United States Government. Neither the United States Government nor any agency thereof, nor any of their employees, makes any warranty, express or implied, or assumes any legal liability or responsibility for the accuracy, completeness, or usefulness of any information, apparatus, product, or process disclosed, or represents that its use would not infringe privately owned rights. Reference herein to any specific commercial product, process, or service by trade name, trademark, manufacturer, or otherwise does not necessarily constitute or imply its endorsement, recommendation, or favoring by the United States Government or any agency thereof. The views and opinions of authors expressed herein do not necessarily state or reflect those of the United States Government or any agency thereof.

**February 1996**

**Prepared for the U.S. Department of Energy  
Under Grant Number DE-FG03-95SF20719**

**DISTRIBUTION OF THIS DOCUMENT IS UNLIMITED**

**MASTER**

## Final Report

### SPECTROSCOPIC DIAGNOSTICS on HIGH-DENSITY, STRONGLY-COUPLED ICF PLASMAS

In our research for the period of February 1, 1995 through November 30, 1995, we have upgraded our equipment in anticipation of the restart of the Omega-Upgrade laser at the University of Rochester Laboratory for Laser Energetics/National Laser User Facility (LLE/NLUF). During the period of this grant we also have completed exploratory experiments on aluminum targets related to both continuum and line emissions near series limits where lines blend into the continuum. This work was performed using the Trident glass laser at Los Alamos National Laboratory. The layout of this experiment showing the diagnostics deployed is shown in Fig. 1. Results were described at the November 1995 meeting of the APS Division of Plasma Physics Conference [1]. We had almost 60 shots at full power [175 J] at  $2\omega$  in 1 ns pulses (Fig. 2) focused to a 0.5-mm diameter spot for an irradiance per beam of  $8 \times 10^{13}$  W/cm<sup>2</sup>. The targets (see also Fig. 1) were mainly 1 mm x 1 mm square aluminum foils of thickness varying from 2.5 to 25  $\mu$ m. Most were coated with 1  $\mu$ m of CH on both sides as a tamper to increase the compressed plasma density prior to expansion. also, most targets were illuminated from both sides.

As highlighted in Fig. 1, we successfully fielded a gated imaging spectrometer (GIS) consisting of a KAP crystal followed by a 4-frame gated x-ray imager. This gave high quality K-shell x-ray line spectra of the hydrogen- and helium-like ions of aluminum, along with an abruptly rising continuum near the  $n=7,8$  lines in the He-like K-shell species (shown in Fig. 3 at a time of 1.4 ns following the beginning of the laser pulse and for a total laser energy of 320 J). This corresponds to an electron density of  $\sim 2.5 \times 10^{21}$  cm<sup>-3</sup>, according to the Inglis-Teller relation [2]. An electron temperature of  $T_e \approx 130$  eV is deduced from relative line intensities in the He-like series for the recombining plasmas. In Fig. 4 is shown a spectrum obtained at somewhat higher laser energy (373 J), at 1.1 ns from the beginning of the laser pulse. The He-like series blends with the continuum at  $n=6$  here, corresponding to an electron density of  $\sim 2 \times 10^{22}$  cm<sup>-3</sup>, which is considerably higher than for Fig. 3. Also apparent in Fig. 4 among the dielectronic satellites on the long wavelength side of the  $n=3-1$  Al XII line is a

line labeled "b", not present in Fig. 3. This results from a  $1s2s3p-1s^22s$  innershell transition (as noted in Figs. 3 and 4 and on the energy level diagram in Fig. 5) normally excited by electron collisions rather than by dielectronic recombination. This explains its absence in Fig. 3, particularly for the low temperature recorded there. We believe that in this case the upper level is "pumped" by collisions from  $1s2p3p$  levels shown in Fig. 5. This occurs at high density when the  $C_{22}$  collisional mixing rate begins to compete with the autoionization rate. Hence, the observation of this particular satellite line relative to others offers a convenient localized indicator of high density in the plasma.

Other density regimes can be pinpointed with other target materials or tracer elements. This satellite density effect has been calculated for a similar transition with a  $n=2$  spectator electron instead of  $n=3$ . A graph of relative intensity versus electron density for this case is shown in Fig. 6, reproduced from Ref. [3]. The presence of this "b" line also occurs if one somewhat artificially assumes that the levels are populated statistically; and such modeling has been done for us by R.C. Mancini at the University of Nevada at Reno as shown in Fig. 7. More precise non-LTE modeling with detailed collisional, radiative and autoionization rates and with kinetics eventually will improve the analysis.

Also, from Figs. 3 and 4, we observe that the  $n=3$  to  $n=1$  transition spectral line for He-like Al XII is more intense than the corresponding line in H-like Al XIII, indicating that the plasma is predominantly in the He-like ion state at our temperatures and densities. Unfortunately any structure (e.g., transparency) in the continuum near the series limit is masked by the  $n=3$  to 1 Lyman- $\beta$  line of hydrogenic Al XIII, as evidenced in Figs. 3 and 4. A similar continuum step in Al XIII at a shorter wavelength (which would not be masked by other lines) could not be observed with this instrument. To eliminate this problem, we plan in future experiments to irradiate similar Mg targets to observe the hydrogenic-ion continuum free of overlapping lines. In Mg XII, this occurs to the short-wavelength side of  $6.5 \text{ \AA}$ , in an ideal spectral region for the present KAP crystal. It is worth mentioning that one component of this spectrograph consisted of a 16-image gated x-ray pinhole camera which we used also to provided snapshots of the plasma.

We also successfully fielded a McPig grazing incidence spectrograph covering 25-1400 Å (oriented as shown in Fig. 1). A sample microdensitometer scan is shown in Fig. 8. From those data we determined that target burn-through from the rear beam became apparent at a thickness of  $\leq 2.5 \mu\text{m}$ . This is important for optimizing target vaporization during the laser pulse for the proposed early-time experiments. Careful microdensitometer scans of the spectrum show evidence of a continuum step for the C V (He-like) and C VI (H-like) 1s-np series (carbon from the coating), as well as Li-like Al XI 2s-np and 2p-nd lines. This continuum step is not unlike that observed for the He-like resonance series in the GIS data described above. McPig spectra obtained at long wavelengths ( $>1000 \text{ \AA}$ ) in these experiments are being examined for evidence of anomalies near the plasma frequency, a subject of a previous proposal.

We also fielded a transmitting-grating spectrograph coupled with a Kentek streak camera for the 0-70 Å spectral region (again, as indicated in Fig. 1). The spectral intensity obtained on this series was insufficient for detailed analysis. Hopefully future experiments with increased sensitivity will yield time-resolved data on any transparency window at the end of the Li-like series limit, as well as useful information on early-time satellite-line features as proposed here.

Similar work is continuing both at LLE (Omega Upgrade) and LANL (Trident), as well as at LLNL (Nova).

#### REFERENCES

1. R.C. Elton, J.A. Cobble, H.R. Griem, G.A. Kyrala, and R.G. Watt, "X-Ray Spectroscopic Diagnostics on TRIDENT", Abstract, APS Div. of Plasma Physics Meeting, Louisville, KY, November 1995, to be published in Bull. Am. Phys. Soc. (1995).
2. H.R. Griem, "Plasma Spectroscopy", p. 125 (McGraw-Hill, NY, 1964).
3. V.L. Jacobs and M. Blaha, Phys. Rev. A **21**, 525 (1980).

# TOP VIEW OF TRIDENT TARGET CHAMBER

TRANS. GRATING &  
STREAK CAMERA

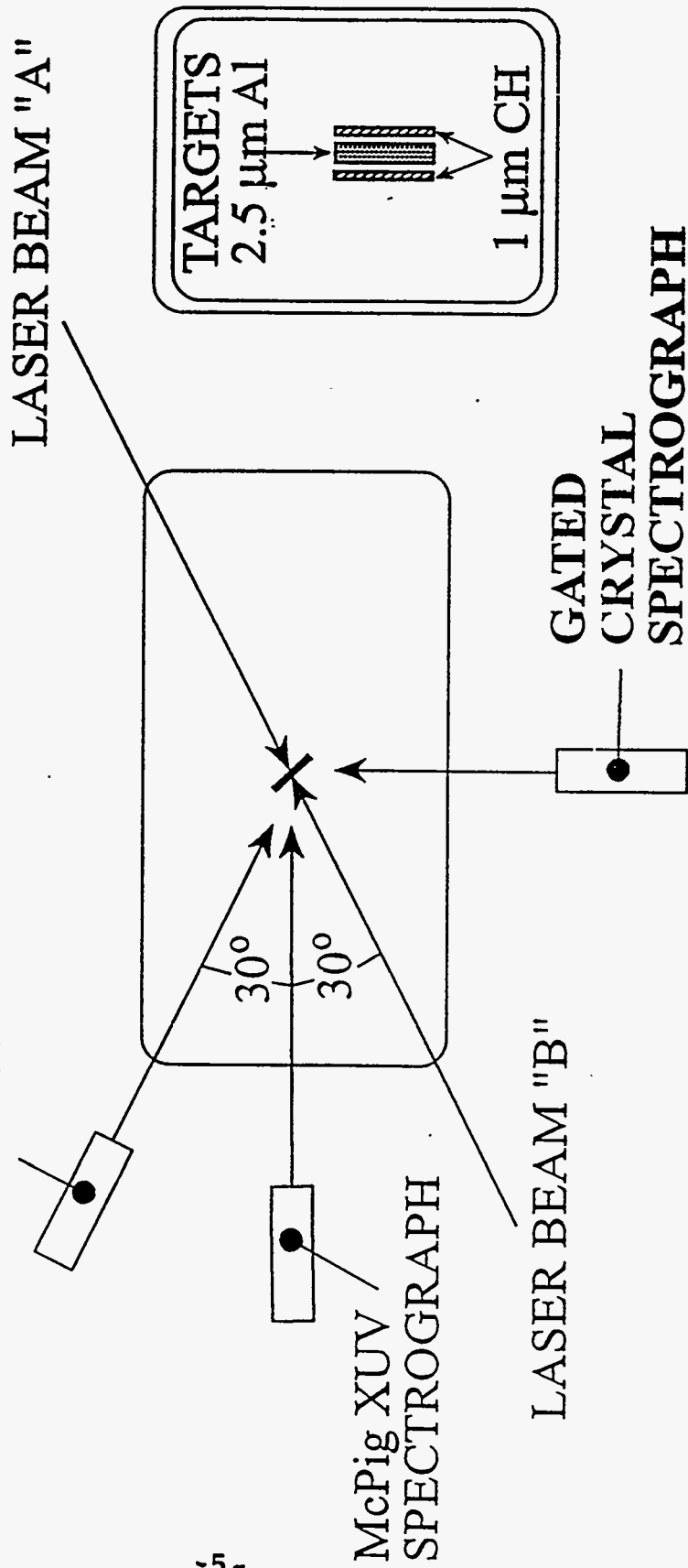


Fig. 1. Layout of the diagnostics fielded on the LANL Trident facility.

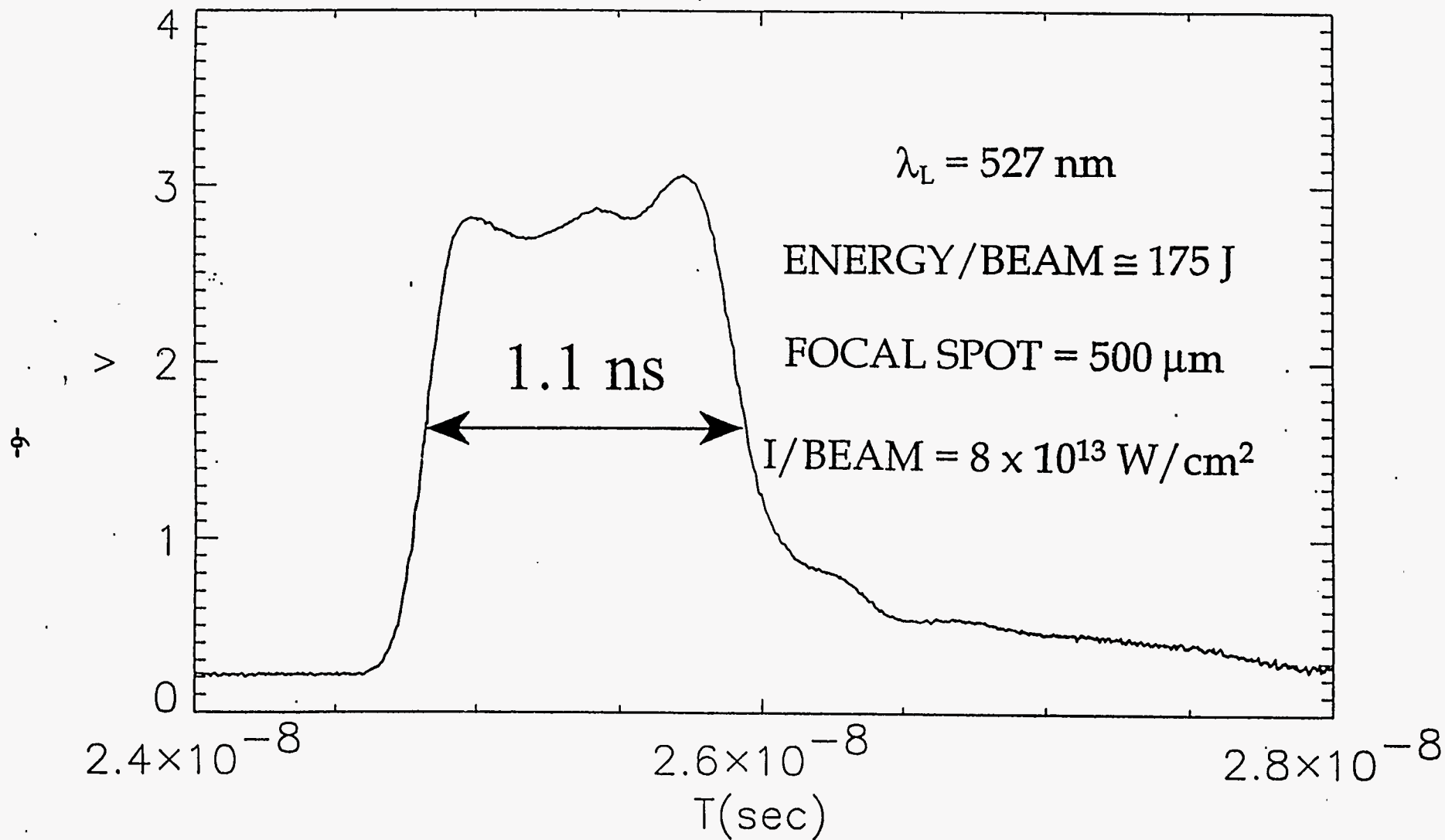


Fig. 2. Typical pulse shape and laser parameters for each of the two beams.

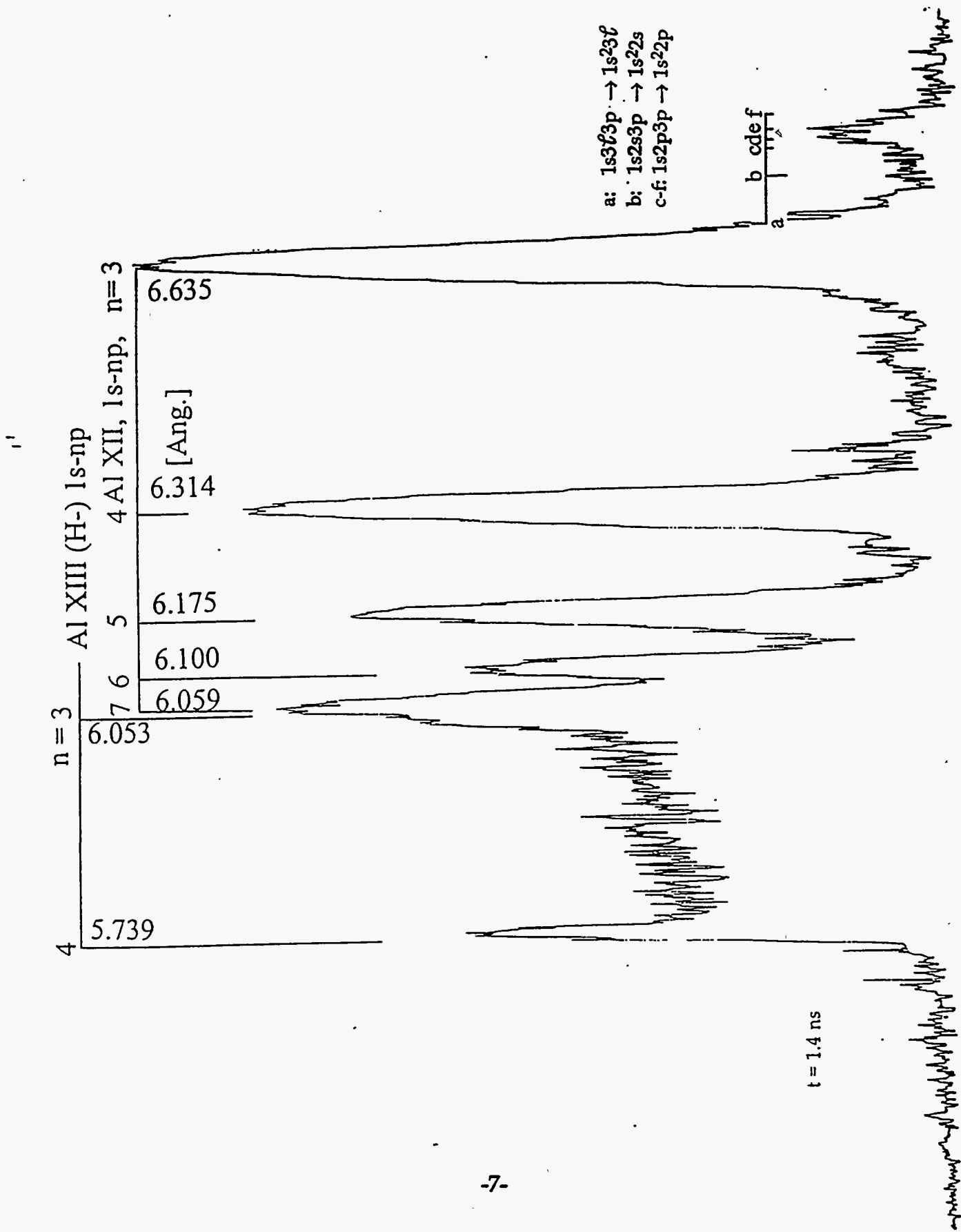


Fig. 3. Microdensitometer tracing from the gated x-ray crystal spectrograph for a

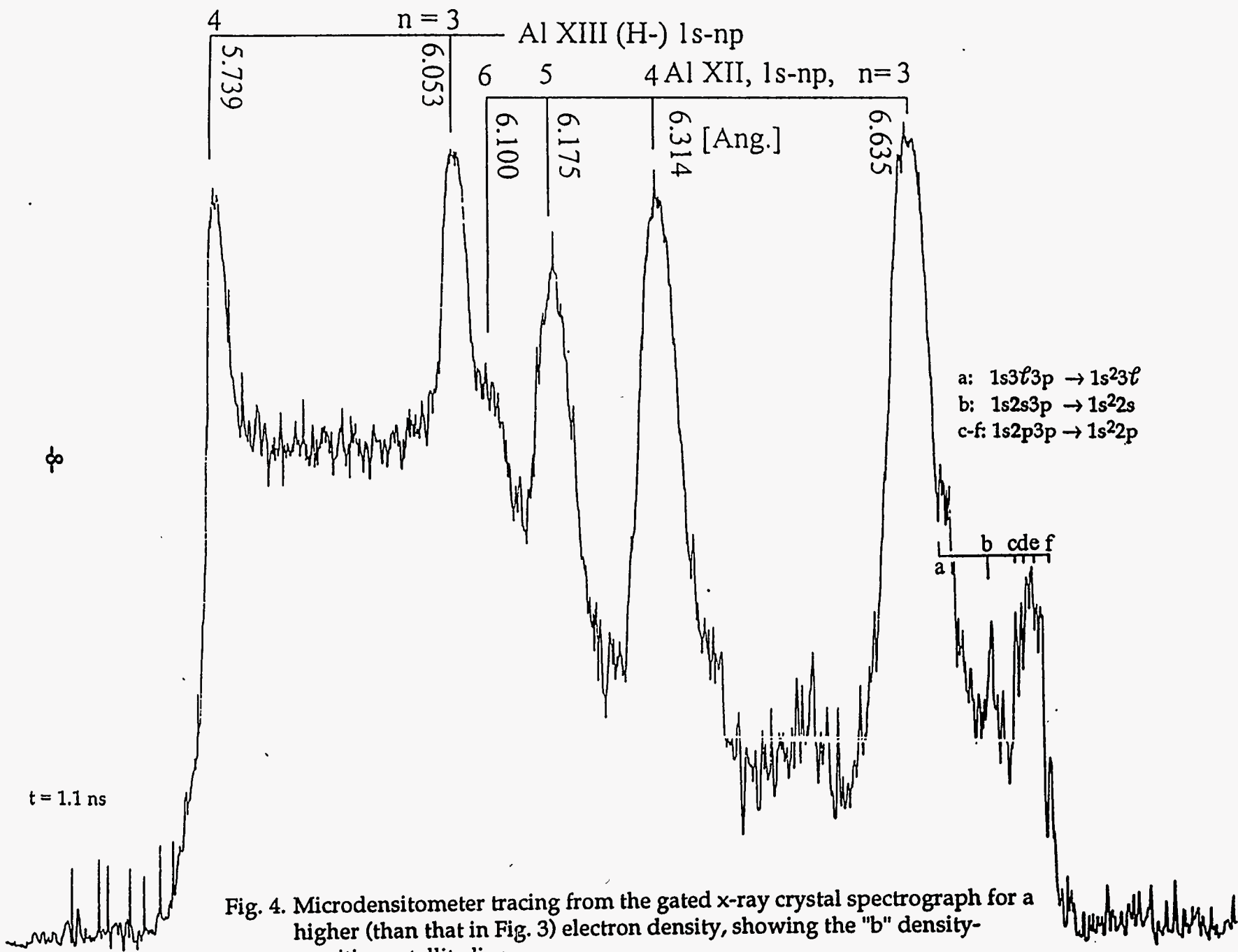


Fig. 4. Microdensitometer tracing from the gated x-ray crystal spectrograph for a higher (than that in Fig. 3) electron density, showing the "b" density-sensitive satellite line.



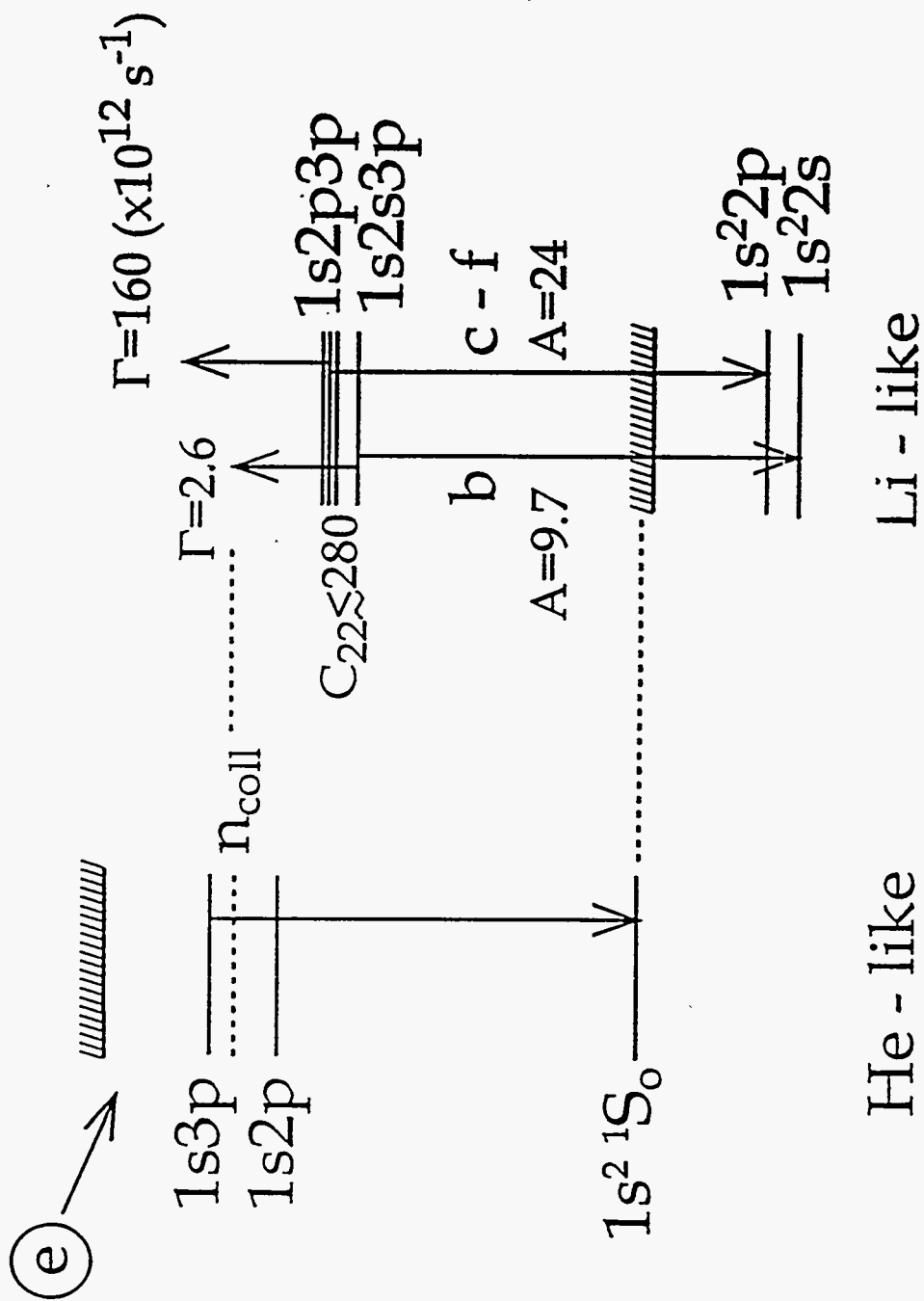


Fig. 5. Energy level and rate diagram showing the satellite transitions and particularly the density-sensitive "b" transition.

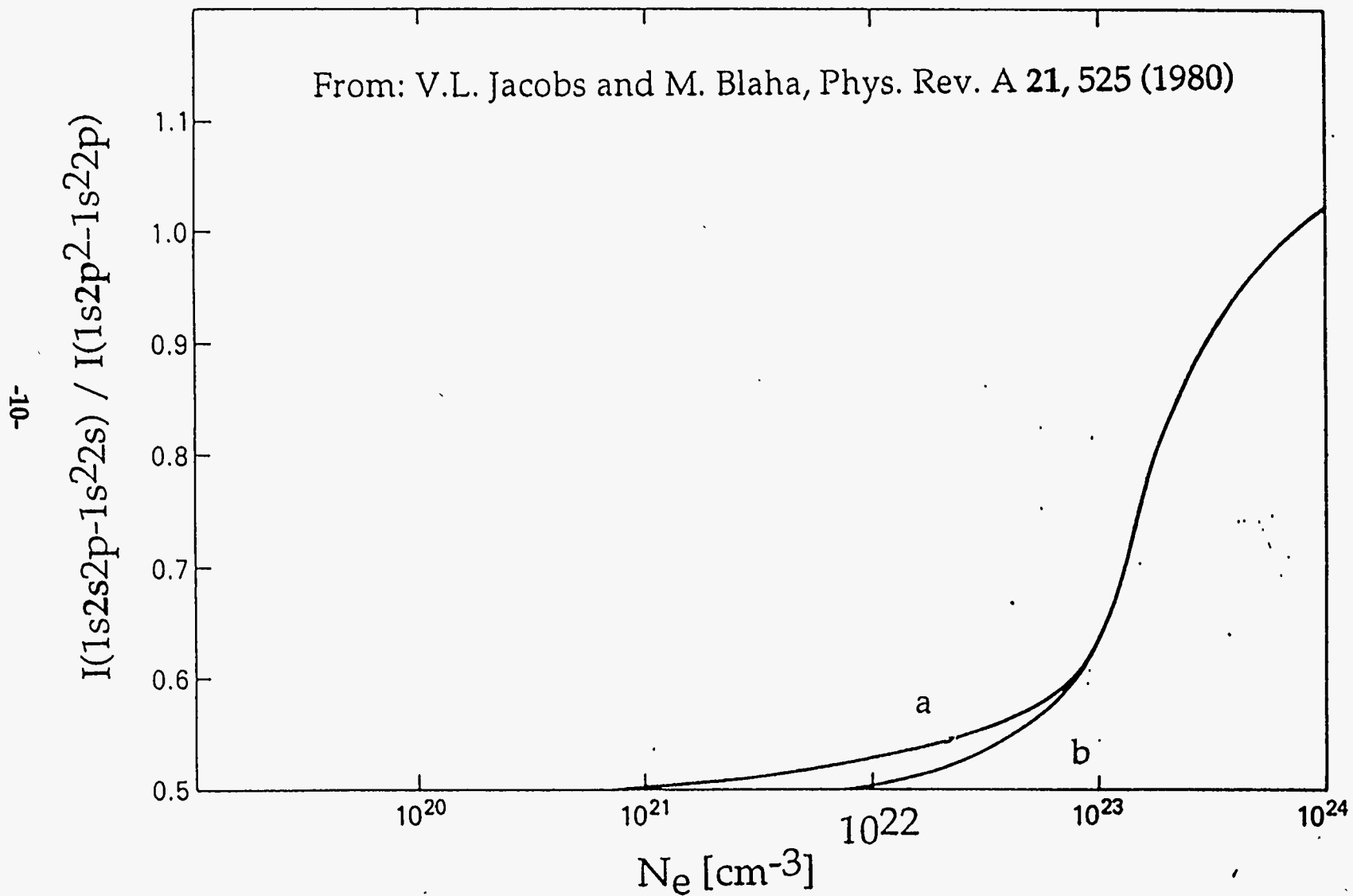


Fig. 6. Relative intensity of satellite lines as a function of electron density.

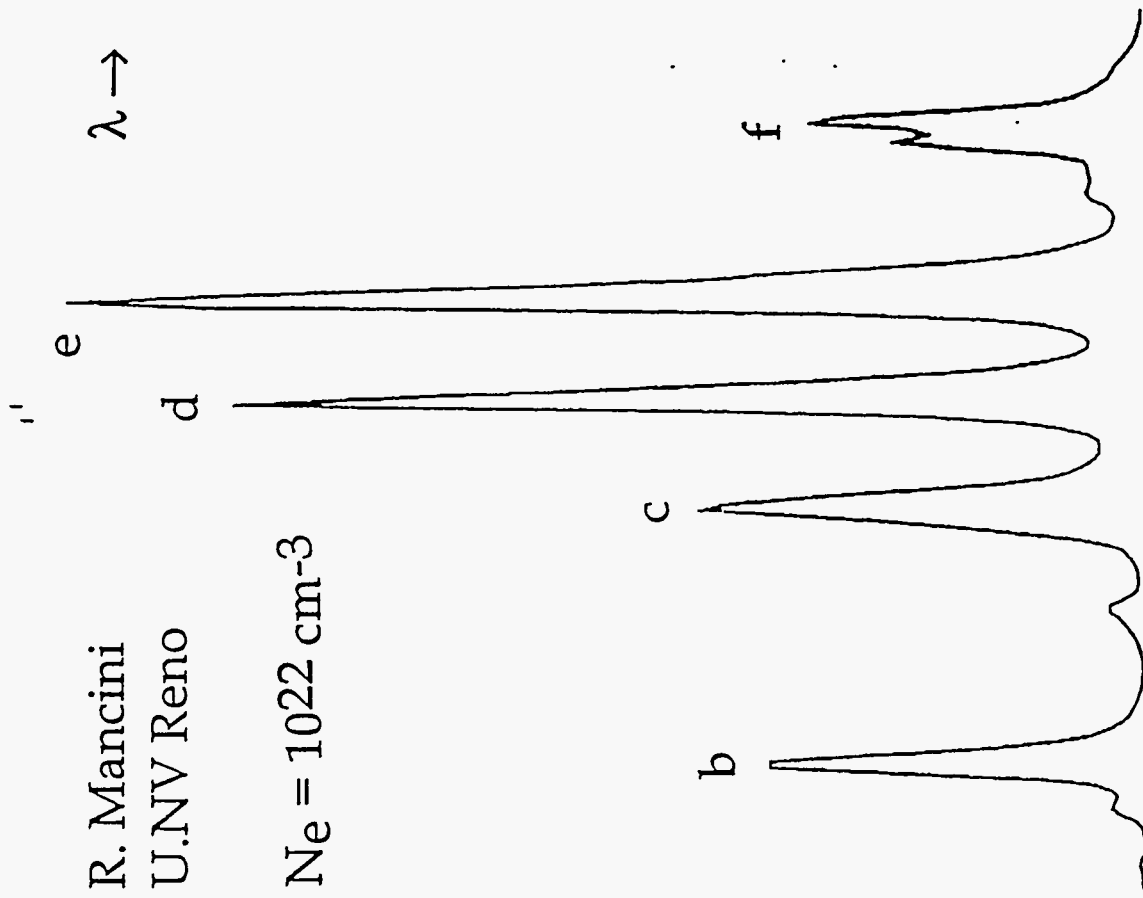


Fig. 7. Numerical calculations of the relative satellite line intensities showing the match to the experimental data in Figs. 3 and 4, assuming here LTE among excited states.

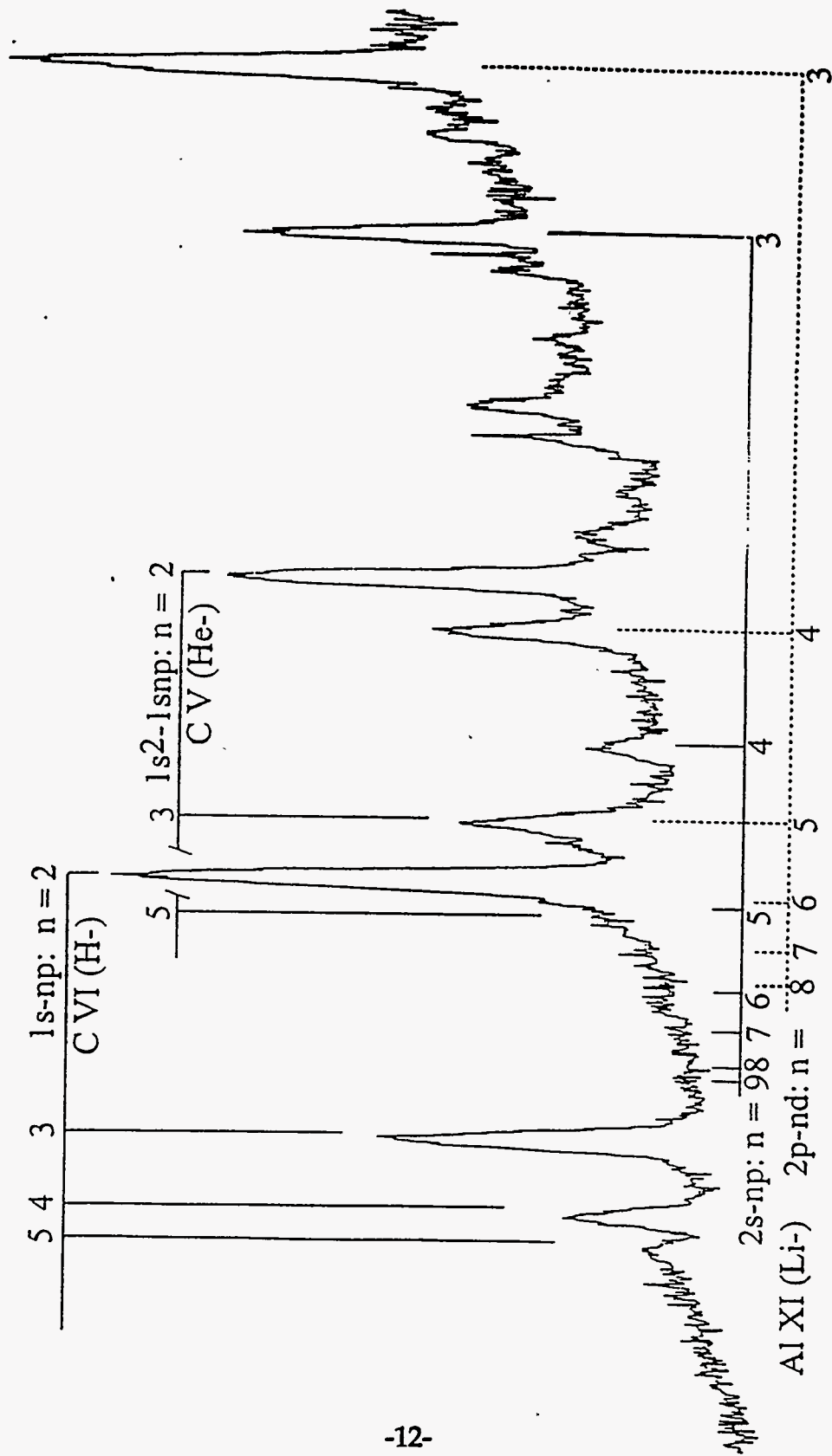


Fig. 8. Microdensitometer scan of a time-integrated spectrum from a McPig grazing-incidence spectrograph.